Demand Response Potential Estimation Model for Typical Industrial Users Considering Uncertain and Subjective Factors

Tingyu Jiang, Member, IEEE, Chuan Qin, Member, IEEE, Yuzhong Gong, Member, IEEE, Ke Wang, Member, IEEE, Ping Ju, Senior Member, IEEE, and Chi Yung Chung, Fellow, IEEE

Abstract-Demand response (DR) is a practical solution to overcoming the challenges posed by the volatility and intermittency of the renewable generation in power systems. Industrial electricity demand is growing rapidly, which makes the DR potential estimation of industrial user critical for the DR implementation. In this paper, a unified model for estimating DR potential in the production processes of aluminum, cement, and steel is proposed on the basis of their unique operational characteristics. Firstly, considering the typical characteristic constraints of different industrial users, a DR potential estimation model is developed to capture typical industrial user response behavior under various operational and economic factors. The proposed estimation model is further refined to account for the uncertain and subjective factors present in the actual estimation environment. Secondly, a virtual data acquisition method is introduced to obtain the private virtual parameters required in the estimation process. Then, an industrial user participation threshold is presented to determine whether industrial users may participate in DR at a given time with consideration of their response characteristics. The industrial users may not always act with perfect rationality, and the response environment remains uncertain. In addition, the subjective factor in this paper includes the proposed threshold and the bounded rationality. Finally, an improved DR potential estimation model is proposed to reduce the difficulties in the actual estimation process. The simulation results validate the effectiveness of the proposed estimation model and the improved DR potential estimation model across multiple cases.

Index Terms—Renewable generation, demand response (DR), industrial user, potential estimation, uncertain factor, subjective factor, unified model.

DOI: 10.35833/MPCE.2024.000764

I. Introduction

EMAND response (DR) aims to incentivize customers to modify their consumption patterns and alleviate the imbalance between electricity supply and demand in an economical and low-carbon manner [1]. The existing DR markets are significant. Approximately 23 GW of DR is available in the U.S. wholesale markets in 2017 [2]. However, one of the key barriers to DR implementation is quantifying the user responsiveness, which is crucial for flexibility aggregation, tariff settlement, and system design [3].

DR potential estimation can be categorized into two types based on direct and indirect estimation methods: baseline estimation and response capability estimation. Baseline estimation is an indirect method used as an intermediate step to estimate the final DR potential.

In [4] and [5], a new closed-loop method and a fully distributed framework based on joint fuzzy C-means are proposed for estimating the aggregated baseline load (ABL) of residential customers. In [6], load data from both before and after the DR-event day are used in the framework proposed in [4] and [5] as the input feature to improve the estimation accuracy. A two-stage decoupled estimation approach to improving the accuracy of ABL estimation in scenarios with behind-the-meter photovoltaic penetration is developed in [7]. DR behaviors of users are constrained and ensured by a selfreported baseline mechanism in [8] and [9]. Based on the state-queueing model, the response capability of fixed airconditioning systems with load adjustment is estimated in [10]. In [11], demand flexibility is quantified by means of time-varying elasticity through Siamese long-short term memory networks.

Previous studies focus on DR potential estimation of residential users. According to IEEE reports, approximately 2%-10% of the industrial users of electricity consume 80% of the total energy production [12]. Industrial users are characterized by high levels of automation and substantial power consumption, making them strong candidates for DR.

DR potential estimation of industrial users is currently divided into two categories: one focuses on modeling the DR potential for specific processes, which emphasizes estimation; and the other involves analyzing the DR potential based on external characteristics, which focuses on scheduling strategies derived from DR potential. The DR potential



Manuscript received: July 19, 2024; revised: October 17, 2024; accepted: January 14, 2025. Date of CrossCheck: January 14, 2025. Date of online publication: March 13, 2025.

This work was supported by the Natural Science Foundation of Jiangsu Province (No. BK20230953), the Joint Funds of the National Natural Science Foundation of China (No. U2066601), and the National Natural Science Foundation of China (No. 52277088).

This article is distributed under the terms of the Creative Commons Attribuion 4.0 International License (http://creativecommons.org/licenses/by/4.0/).

T. Jiang, C. Qin (corresponding author), K. Wang, and P. Ju are with the School of Electrical and Power Engineering, Hohai University, Nanjing, China (e-mail: jtingyuyuki@163.com; cqin@hhu.edu.cn; 20220021@hhu.edu.cn; pju@hhu.edu.cn;

Y. Gong is the College of Control Science and Engineering, Zhejiang University, Hangzhou, China (e-mail: yzgong@zju.edu.cn).

C. Y. Chung is with the Department of Electrical Engineering, The Hong Kong Polytechnic University, Hong Kong, China (e-mail: c.y.chung@polyu.edu. hk)

in energy-intensive industries in Germany is investigated in [13], which emphasizes the need for tailored strategies. In [14], a thermo-economic analysis of heat-driven ejectors for cooling in smelting processes is performed to assess the DR potential. Reference [15] evaluates the flexibility potential of two energy-intensive industries, which are the chlor-alkali process and wood pulp production. In [16], the energy-efficient scheduling of steel plants with flexible electric arc furnaces centers is formulated to minimize costs based on dynamic electricity pricing. In [17], the DR potential of oxygen production and thermostatic equipment in aquaculture is estimated to provide constraints for reducing the operational power costs.

The focus of the above studies lies in the DR potential estimation. In contrast, DR potential is primarily used to support scheduling in the following studies. In [18], a DR trade model that addresses cost and revenue allocation in hydrogen-to-electricity conversion is developed. In [12], the power consumption modeling for production processes is proposed, which focuses on supporting day-ahead scheduling with DR. In [19], a data-driven real-time price-based DR management scheme is proposed for industrial energy facilities. In [20] and [21], the DR potential is estimated based on power characteristics and incorporated into the scheduling model. In addition, an hour-ahead price-based energy management scheme is proposed to dynamically adjust industrial power consumption in [22].

Studies on DR potential estimation of industrial users remain limited because of their insufficient willingness to participate in DR and the necessity of maintaining normal production. The current challenges in the DR potential estimation of industrial users are as follows.

- 1) DR potential estimation of industrial users must consider the coordination in various production processes rather than treating them independently.
- 2) Participation of industrial user in DR is fundamentally an economic decision. To understand the user psychology in the response process, it requires the consideration of both the uncertain and subjective factors.
- 3) DR potential estimation of industrial users varies greatly across different industrial consumers. Hence, it is essential to establish a unified model to ensure the standardization and usability of the estimated DR potential.

In this context, a unified DR potential estimation model is proposed to estimate the DR potential of typical industrial users. The main contributions of this study are as follows.

- 1) A unified DR potential estimation model for typical industrial users is formulated considering operational and economic factors, which is standardized and easily expandable.
- 2) Different from that for DR of residential users, an industrial user participation threshold is proposed to evaluate whether the industrial user participates in DR.
- 3) Considering the uncertain and subjective factors in the estimation process, an improved DR potential estimation model is further proposed to increase its practical applicability.

The structure of the remainder of this paper is as follows. Section II presents the basic analysis. Section III introduces the proposed estimation model for typical industrial users.

Section IV shows the improved DR potential estimation model considering uncertain and subjective factors. Case study and conclusions are provided in Sections V and VI, respectively.

II. BASIC ANALYSIS

The accurate DR potential estimation of industrial users enables the distribution system operator (DSO) to schedule DR resources effectively, thereby promoting the normalization and large-scale implementation of DR. The difference between DR potential estimation and response scheduling is that the former represents the maximum willingness to response, rather than the actual response amplitude.

Industrial users are rational and adjust their willingness to response based on the incentive price. Thus, DR potential estimation must account for economic factors. Furthermore, there are uncertain and subjective factors in the actual estimation process that must be considered. These two issues are addressed in Sections III and IV, respectively.

A. Framework

Figure 1 illustrates the framework of the proposed estimation model, where ASP is short for aluminum smelting plant; CMP is short for cement manufacturing plant; and SMP is short for steel manufacturing plant. In the day-ahead stage, the DSO communicates response requirements to industrial users. Industrial users estimate their optimal DR capacity and report it to the DSO with uncertain incentives. In the intraday stage, the DSO determines the incentive price based on the actual source-load situation and aggregated response capacities. This paper focuses on the unified DR potential estimation model during the day-ahead stage.

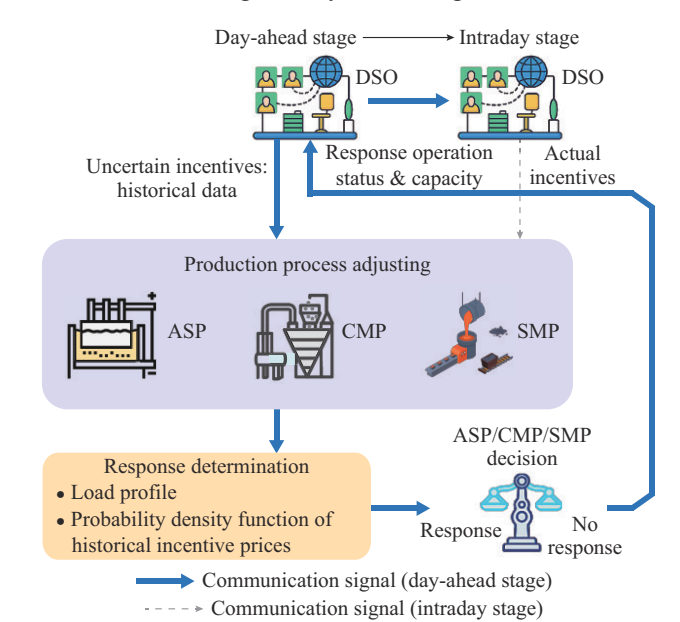


Fig. 1. Framework of proposed estimation model.

The power consumption of industrial users can be divided into production consumption and nonproduction consumption. Production consumption is primarily associated with machine-driven processes, electric heating, and other related activities. These activities support industrial production needs, some of which follow a specified sequence that cannot be interrupted. The objective of the DR potential estimation in this paper is the production consumption, as it accounts for the majority of the energy consumed in industrial production.

Figure 2 illustrates the schematic diagram of the proposed estimation model. Firstly, the impacts of power consumption patterns (workdays and nonworkdays), as well as the correlation between the electricity price and the load curve, are analyzed to provide a theoretical basis for subsequent modeling. Secondly, the proposed estimation model is established, with heterogeneous constraints derived from the production characteristics of different typical industrial users. Finally, an improved DR potential estimation model is proposed considering the difficulty in obtaining private information, the uncertainty information, and the response characteristics of industrial users.

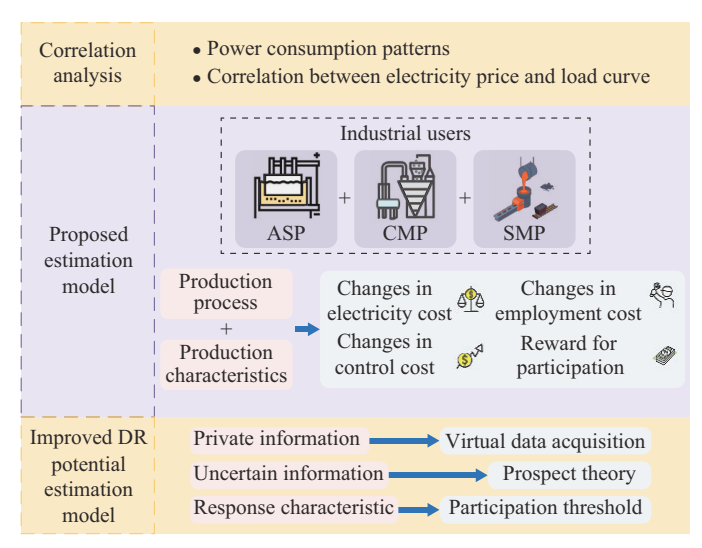


Fig. 2. Schematic diagram of proposed estimation model.

B. Correlation Analysis of Workdays v.s. Nonworkdays

The accuracy of the proposed estimation model is significantly influenced by the operation status of industrial users. The most obvious and common factor influencing the operation status of industrial users is whether the day is a workday.

Two indices are used to assess the similarity between the power consumption patterns on workdays and nonworkdays: the power consumption amplitude and the similarity of the load curves. The power consumption amplitude can be easily accessed through curve classification, whereas the similarity of load curves must be evaluated via a specific method. Notably, the Hausdorff distance (HD) is introduced to judge the similarity of line shapes [23], [24]. The HD measures the distance between two subsets of a metric space. The smaller the HD, the more similar the lines are, which indicates a stronger correlation between them. The definition of HD and related formulas are shown in Supplementary Materia A. The average HD between workday load curves and nonworkday load curves \overline{H}_{P_L} is calculated through (SA5) in Supplementary Materia A.

The electricity price has an important effect on the operation of industrial production, causing the load to fluctuate regularly with changes in the electricity price. However, the actual load curve does not exhibit a sharp contrast between high power consumption period and low power consumption period, i.e., the operation status of the industrial user is also significantly affected by other factors. Therefore, the correlation between the electricity price and the load curve should be analyzed to provide a foundation for the subsequent modeling. HD is used to assess the similarity between the electricity price and the load curve. The average HD between the electricity price and the load curves \overline{H}_{L_p} is shown in (SA6) in Supplementary Materia A.

The results indicate that the correlation between electricity price and load curves is significantly weaker than the correlation between workday load curves and nonworkday load curves. Overall, the daily operation status of industrial users remains relatively stable, and electricity cost does not serve as a decisive factor influencing the operation status of industrial users.

III. PROPOSED ESTIMATION MODEL FOR TYPICAL INDUSTRIAL USERS

Typical industrial users are selected for DR potential estimation, e.g., ASP, CMP, and SMP. The aforementioned industrial users are typical high power-consuming industries with a high level of automation. Moreover, the production processes of these industrial users and their corresponding regulation methods exhibit substantial variations in flexibility, energy consumption, and other aspects. These processes encompass most industrial production lines and reflect the universality of industrial users.

The DR potential provided by industrial users is driven by economic factors. By optimizing the economic cost alterations related to adjusting the operation status of the internal equipment to participate in DR C_s , the optimal DR potential can be determined. Therefore, a unified DR potential estimation model for industrial users is developed, comprising three components: a unified objective function, general constraints, and heterogeneity constraints. The heterogeneity constraints account for the distinct production processes and response requirements of various industrial users. The unified objective function is formulated as (1). The weight coefficient λ_s is used to reduce the impact of changes in electricity cost and adhere to the principles of industrial production. Consequently, it prevents industrial users from concentrating their power consumption during the valley period. Otherwise, the optimization results are only theoretically optimal and do not satisfy the actual industrial production demand.

$$\min C_s = \lambda_s \Delta C E_s + \Delta C C_s + \Delta C S_s - R E_s \tag{1}$$

where subscript s is the element of set $S=\{ASP,CMP,SMP\};$ ΔCE_s is the change in electricity cost; ΔCC_s is the change in control cost; ΔCS_s is the change in employment cost; and RE_s is the revenue for participation in DR.

General constraints include the conservation in relation to production goals (i.e., energy conservation) and the requirement of adhering to the original production operation scheme. In contrast, heterogeneity constraints account for specific equipment switching methods, storage requirements, and other operational limitations. Required inputs and outputs of the estimation model are provided in Remark SA1 of Supplementary Material A.

Remark 1: why do we use a unified model to estimate the DR potential of industrial users?

The unified DR potential estimation model proposed in this paper encompasses typical production processes. It facilitates DR potential estimation of industrial users on a unified basis and is easier to generalize in the context of regional and multi-industry DR potential estimation. The differences in DR potential among industrial users are reflected in the constraint conditions.

Based on field research, the following assumptions are made to simplify the modeling process.

Assumption 1: the production rate is proportional to power consumption.

Assumption 2: identical types of industrial production equipment share the same parameters.

The discussions regarding the validity and limitations of Assumptions 1 and 2 are provided in Remarks SA2 and SA3 of Supplementary Material A, respectively. It is worth noting that the unified DR potential estimation model corresponds to the proposed estimation model.

A. Proposed Estimation Model for ASP

In the aluminum smelting process, alumina is converted into aluminum, thus providing material for various industries. The production process of an ASP mainly includes bauxite mining, alumina production, anode preparation, electrolytic aluminum production, and aluminum ingot casting stages. The power consumption in each stage accounts for 1%, 21%, 2%, 74%, and 2%, respectively. Therefore, the electrolytic aluminum process is adjusted to provide DR capacity, and its DR potential is estimated.

Electrolytic aluminum production process is initiated in pots under low DC voltage. Hundreds of cells are connected in series to form a potline or multiple potlines. The power consumption of a potline is high, and it has sufficient flexibility to response rapidly to the increase or decrease in energy demands. Generally, there are two ways to adjust the power consumption of a potline:

- 1) Turn the pot on/off. Since the pot operation requires strict thermal balance, this way negatively impacts the electrolytic aluminum process.
- 2) Adjust the tap changers in the rectifier stations. The tap positions can change quickly and accurately, allowing for rapid reduction or increase in power consumption, as demonstrated in Alcoa's Warrick operation [25]. This way is selected because it exerts less impact on the production process.

The proposed estimation model for an ASP is given by (2). We assume that there are $n_{\rm ASP}$ pots that can be adjusted (a potline) and each pot has K tap positions. The power consumption of the $i^{\rm th}$ pot $P_{{\rm ASP},i,t}$ and the potline in an ASP after and before rescheduling $P_{{\rm ASP},t}$ and $P_{{\rm ASP},t,0}$ are derived in (3)-(5).

$$\min C_{\text{ASP}} = \lambda_{\text{ASP}} \Delta C E_{\text{ASP}} + \Delta C C_{\text{ASP}} + \Delta C S_{\text{ASP}} - R E_{\text{ASP}}$$
 (2)

$$P_{\text{ASP},i,t} = \sum_{k=1}^{K} z_{i,t,k} P_{\text{ASP},k}$$
 (3)

$$P_{ASP,t} = \sum_{i=1}^{n_{ASP}} \sum_{k=1}^{K} z_{i,t,k} P_{ASP,k}$$
 (4)

$$P_{\text{ASP},t,0} = \sum_{i=1}^{n_{\text{ASP}}} \sum_{k=1}^{K} z_{i,t,k_0} P_{\text{ASP},k_0}$$
 (5)

where the subscript k is the tap position; the subscript k_0 is the tap position at the original operation point; and $z_{i,t,k}$ is the i^{th} pot in the k^{th} tap position with the power consumption $P_{\text{ASP},k}$ at time t.

 $\Delta CE_{\rm ASP}$ and $\Delta CC_{\rm ASP}$ are calculated in (6) and (7) and are obtained by subtracting the cost of the original operation point from the cost of the rescheduled operation point. Excessive switching of machines may accelerate the degradation and potentially cause damage. Therefore, switching actions are penalized.

$$\Delta CE_{ASP} = \sum_{t=1}^{T} EP_{t} \sum_{i=1}^{n_{ASP}} \sum_{k=1}^{K} (z_{i,t,k} P_{ASP,k_{0}} - z_{i,t,k_{0}} P_{ASP,k_{0}})$$
 (6)

$$\Delta CC_{\text{ASP}} = \sum_{t=2}^{T} \sum_{i=1}^{n_{\text{ASP}}} \sum_{k=1}^{K} C_{\text{ASP}} |z_{i,t,k} - z_{i,t-1,k}| - \sum_{t=2}^{T} \sum_{i=1}^{n_{\text{ASP}}} \sum_{k=1}^{K} C_{\text{ASP}} |z_{i,t,k_0} - z_{i,t-1,k_0}|$$
(7)

where T is the number of time intervals; and EP_t is the electricity price at time t.

The changes in employment cost $\Delta CS_{\rm ASP}$ is associated with starting and stopping the potline. A certain number of workers are required to supervise production when the potline operates normally. In the response process, the on/off status of the potlines remain unchanged. Hence, as shown in (8), $\Delta CS_{\rm ASP}$ is set to be 0. The DR is set to activate at t_1 and t_2 . The obtained revenue can be deduced with (9), and the duration of t_1 and t_2 is set to be 0.5 hour.

$$\Delta CS_{\rm ASP} = 0 \tag{8}$$

$$RE_{ASP} = w_1 | P_{ASP,t_1} - P_{ASP,t_2,0} | + w_2 | P_{ASP,t_3} - P_{ASP,t_3,0} |$$
 (9)

where w_1 and w_2 are the incentive coefficients.

Several constraints are considered. As specified in (10), the pot must be switched to a specific tap position to maintain thermal balance and avoid interfering with normal production. The production target of electrolytic aluminum is ensured through the equal power consumption constraint in (11). Furthermore, changing the tap positions too frequently within the same pot may shorten its service life. According to (12), within every four consecutive time slots, the tap position can be switched at most once.

$$\sum_{k=1}^{K} z_{i,t,k} = 1 \tag{10}$$

$$\sum_{t=1}^{T} P_{ASP,t} = \sum_{t=1}^{T} P_{ASP,t,0}$$
 (11)

$$|z_{i,t,k} - z_{i,t-1,k}| + |z_{i,t-1,k} - z_{i,t-2,k}| + |z_{i,t-2,k} - z_{i,t-3,k}| \le 1$$
 (12)

The typical production states of an ASP can be categorized into the rated production, reduced production, holding, and cooling states, which switch according to the DC bus current. In the rated production state, the DC current of the pot is between 90% and 100% of the rated value. In the reduced production state, aluminum electrolysis can still pro-

ceed normally, but the output of aluminum liquid decreases due to reduced energy input. In the holding and cooling states, maintaining normal production of aluminum electrolysis proves to be difficult and may even lead to equipment damage. Therefore, the current of aluminum electrolysis is constrained to ensure normal production. Equations (13) and (14) calculate the DC current $I_{\text{d,i,t,k}}$ and DC voltage $V_{\text{B,i,t,k}}$ of the i^{th} pot in the k^{th} tap position at time t, respectively. Equation (15) limits the allowable fluctuation range of $I_{\text{d,i,t,k}}$ through switching the tap changers in the rectifier stations.

$$I_{d,i,t,k} = V_{B,i,t,k} - \frac{E}{R_{EC}}$$
 (13)

$$V_{B,i,t,k} = 1.35 \left(\frac{V_{AL}}{TAP_{i,t,k}} - V_{SR} \right)$$
 (14)

$$0.9 \le \frac{I_{d,i,t,k}}{I_{d0}} \le 1.0 \tag{15}$$

where $R_{\rm EC}$ and E are the equivalent resistance on the load DC side and the back electromotive force, respectively; $V_{\rm AL}$ and $V_{\rm SR}$ are the high-voltage bus voltage on the load side and the voltage drop across the saturable reactor, respectively; $TAP_{i,t,k}$ is the voltage transformation ratio of the $i^{\rm th}$ pot in the $k^{\rm th}$ tap position at time t, which corresponds to $z_{i,t,k}$; and $I_{\rm d0}$ is the rated DC current of a pot.

Furthermore, the primary purpose of rescheduling the operation point of an ASP is to generate revenue while providing DR resources, rather than optimizing the operational configuration for revenue. Therefore, with the exception of t_1 and t_2 , the power consumption must fluctuate near the initial curve. In addition, the power consumption should not be excessively biased toward the periods of low electricity prices, thereby preventing the distortion of its original pattern. Equation (16) illustrates this rule, and the response range at t_1 and t_2 is constrained by (17).

$$P_{\text{ASP},t,0} - \delta_{\text{ASP}} \le P_{\text{ASP},t} \le P_{\text{ASP},t,0} + \delta_{\text{ASP}} \quad t \in \mathbb{T} \setminus \{t_1, t_2\} \quad (16)$$

$$P_1 \le P_{ASP,t} - P_{ASP,t,0} \le 0 \qquad \forall t = t_1, t_2$$
 (17)

where δ_{ASP} is the allowable range of power variation of ASP; $\mathbb{T} = \{1, 2, ..., T\}$; and P_1 is the maximum regulation amplitude.

B. Proposed Estimation Model for CMP

Cement production is an energy-intensive industry, with power consumption representing approximately 30% of its total costs. The cement production process involves four main stages: crushing (CR), kiln feed preparation (KFP), clinker production (CP), and finish grinding (FG) stages. The KFP stage must remain in operation due to its large thermal capacity. In addition, the cost of turning the kiln on or off is high. Although other stages can be interrupted, the CP stage is characterized by relatively low flexibility and produces hot clinker, which is cooled and fed into the FG stage for grinding into cement powder. The CP and FG stages are coupled through the clinker storage area, whose capacity is smaller than that of the raw material storage area. Therefore, the FG stage must operate continuously to prevent the clinker accumulation. The most suitable process for interruption is the CR stage. In the CR stage, a rapid on/off switching is adopted to quickly adjust the power consumption, specifically by turning the crushers on or off.

The proposed estimation model for a CMP is given by (18). Given that there are n_{CMP} crushers that can be adjusted, a binary variable $\mu_{m,t}$ is introduced to denote the operation status of the m^{th} crusher at time t. $\mu_{m,t} = 1$ represents that the crusher is on, and $\mu_{m,t} = 0$ represents that the crusher is off. The power consumption of the m^{th} crusher $P_{\text{CMP},m,t}$ and all adjustable crushers in a CMP after and before rescheduling $P_{\text{CMP},t,0}$ are derived in (19)-(21).

$$\min C_{\text{CMP}} = \lambda_{\text{CMP}} \Delta C E_{\text{CMP}} + \Delta C C_{\text{CMP}} + \Delta C S_{\text{CMP}} - R E_{\text{CMP}}$$
 (18)

$$P_{\text{CMP},m,t} = \phi_m \mu_{m,t} \tag{19}$$

$$P_{\text{CMP},t} = \sum_{m=1}^{n_{\text{CMP}}} \phi_m \mu_{m,t}$$
 (20)

$$P_{\text{CMP},t,0} = \sum_{m=1}^{n_{\text{CMP}}} \phi_m \mu_{m,t}^0$$
 (21)

where ϕ_m is the rated power of the m^{th} crusher; and $\mu_{m,t}^0$ is the original operation status of the m^{th} crusher at time t.

Similarly, $\Delta CE_{\rm CMP}$ and $\Delta CC_{\rm CMP}$ are calculated in (22) and (23), respectively. The difference between the CMP and ASP is that the CMP uses on/off switching to adjust power consumption, and there is a difference in labor costs between day and night shifts. Therefore, the changes in labor costs must be taken into account in (24). Finally, the received revenue of the CMP $RE_{\rm CMP}$ can be calculated in (25).

$$\Delta CE_{\text{CMP}} = \sum_{t=1}^{T} EP_{t} \sum_{m=1}^{n_{\text{CMP}}} (\phi_{m} \mu_{m,t} - \phi_{m} \mu_{m,t}^{0})$$
 (22)

$$\Delta CC_{\text{CMP}} = \sum_{t=2}^{T} \sum_{m=1}^{n_{\text{CMP}}} C_{\text{CMP}} |\mu_{m,t+1} - \mu_{m,t}| - \sum_{t=2}^{T} \sum_{m=1}^{n_{\text{CMP}}} C_{\text{CMP}} |\mu_{m,t+1}^{0} - \mu_{m,t}^{0}|$$
(23)

$$\Delta CS_{\text{CMP}} = C_{\text{SA}} \sum_{t=1}^{T} \sum_{m=1}^{n_{\text{CMP}}} |\mu_{m,t} - \mu_{m,t}^{0}|$$
 (24)

$$RE_{\text{CMP}} = w_1 | P_{\text{CMP}, t_1} - P_{\text{CMP}, t_1, 0} | + w_2 | P_{\text{CMP}, t_2} - P_{\text{CMP}, t_2, 0} |$$
 (25)

where $C_{\rm CMP}$ is the cost coefficient for the switching action of the CMP; and $C_{\rm SA}$ is the salary coefficient.

Since the CMP operates at rated power in the CR stage, the output rate of raw materials remains constant when it is on, as shown in (26). Therefore, the normal production process can be maintained with the same power consumption in the CR stage.

$$\sum_{t=1}^{T} P_{\text{CMP},t} = \sum_{t=1}^{T} P_{\text{CMP},t,0}$$
 (26)

In the cement production process, the CR and KFP stages are connected through the raw material storage area. The KFP stage is always on with a constant consumption rate. Thus, the amount of the stored intermediate product is directly related to the number of crushers in operation. To increase the flexibility of the CMP in transferring the load, all crushers are considered to share a single storage area, as shown in (27). However, the storage-area capacity is limited. The operation status of the crushers must be carefully man-

aged to prevent overflow or insufficient storage in the KFP stage, as specified in (28).

$$q_t + \sum_{m=1}^{n_{\text{CMP}}} B_{\text{p}} \mu_{m,t} - \tau_{\text{C}} = q_{t+1}$$
 (27)

$$Q_{\text{low}} \le q_t \le Q_{\text{high}} \tag{28}$$

where q_t is the utilization volume of the storage area at time t; B_p and τ_C are the generation rate of the CR stage and the consumption rate of the KFP stage, respectively; and Q_{low} and Q_{high} are the lower and upper limits of the storage area, respectively.

Finally, the response ranges at t_1 and t_2 are constrained in (29) and (30), respectively.

$$P_{\text{CMP},t,0} - \delta_{\text{CMP}} \leq P_{\text{CMP},t} \leq P_{\text{CMP},t,0} + \delta_{\text{CMP}} \quad t \in \mathbb{T} \setminus \{t_1, t_2\} \tag{29}$$

$$P_2 \le P_{\text{CMP},t} - P_{\text{CMP},t,0} \le 0 \quad \forall t = t_1, t_2$$
 (30)

where $\delta_{\rm CMP}$ is the allowable range of power variation of CMP; and P_2 is the maximum regulation amplitude.

C. Proposed Estimation Model for SMP

In contrast to aluminum smelting, steel manufacturing involves a complex production process, where both logistics management and energy optimization are crucial. Given that the objective is not to optimize the production of the steel plant, only power consumption is considered in this context.

The production process of SMP includes four equipment: electric arc furnace (EAF), argon oxygen decarburization (AOD), ladle furnace (LF), and continuous caster (CC). The first three equipment operate in batch mode, meaning a specified amount of metal is processed at a time [23]. Each batch of metal is called one heat. One heat is generated in the EAF, and the generated heat is subsequently transported to the AOD to reduce the carbon content. In the LF, the specific parameters of the liquid steel are adjusted, and this liquid steel is cast into slabs in the CC.

The most power-intensive production stage occurs in the EAF. Moreover, the scrap metal begins to cool after an interruption lasting more than 30 min. Furthermore, restarting melting process incurs additional costs. Since EAFs are powered by transformers, their power consumption can be adjusted by changing the position of the on-load tap changers (OLTCs). However, frequent switching of the OLTCs may reduce their lifetime.

1) Typical Distinction Illustration

The SMP is selected as the third typical industrial user due to the continuity of its production process. As mentioned earlier, one heat is generated in an EAF, but the total energy required for melting is fixed, and the melting process cannot be interrupted. In other words, the product of the melting duration and the melting power equals a constant value.

Since the melting process cannot be interrupted, the setting of OLTC cannot be altered while the melting is in progress. In other words, the setting of the OLTC must remain fixed, and the corresponding fixed duration depends on the tap setting. For ASP, electrolytic aluminum production operates continuously, which means that the switching of the tap position can occur at any time and only affects the output rate rather than the final result.

For different melting modes, the melting task for each mode fully spans the current time slot. The time slot is set to be 0.5 hour. If the melting time of a mode is 79 min, it is viewed as spanning 3 time slots.

2) Proposed Estimation Model Formulation

The proposed estimation model for an SMP is given in (31). Given that there are n_{SMP} EAFs that can be adjusted and each EAF has H tap positions. The power consumption of the j^{th} EAF $P_{\text{SMP},j,t}$ and all the EAFs in an SMP after and before rescheduling $P_{\text{SMP},t}$ and $P_{\text{SMP},t,0}$ are derived in (32)-(34).

$$\min C_{\text{SMP}} = \lambda_{\text{SMP}} \Delta C E_{\text{SMP}} + \Delta C C_{\text{SMP}} + \Delta C S_{\text{SMP}} - R E_{\text{SMP}}$$
 (31)

$$P_{\text{SMP},i,t} = z_{i,t,h} P_{\text{SMP},h} \tag{32}$$

$$P_{\text{SMP},t} = \sum_{j=1}^{n_{\text{SMP}}} \sum_{h=1}^{H} z_{j,t,h} P_{\text{SMP},h}$$
 (33)

$$P_{\text{SMP},t,0} = \sum_{i=1}^{n_{\text{SMP}}} \sum_{h=1}^{H} z_{j,t,h_0} P_{\text{SMP},h_0}$$
 (34)

where $P_{\text{SMP},h}$ is the power consumption of SMP in the h^{th} tap position; $z_{j,t,h}$ is the j^{th} EAF in the h^{th} tap position with power consumption at time t; and the subscript h_0 denotes the tap position at the original operation point.

 $\Delta CE_{\rm SMP}$, $\Delta CC_{\rm SMP}$, and $\Delta CS_{\rm SMP}$ are calculated in (35)-(37), respectively. DR is set to activate at t_1 and t_2 . The received revenue of the SMP $RE_{\rm SMP}$ is calculated in (38).

$$\Delta CE_{\text{SMP}} = \sum_{t=1}^{T} EP_{t} \sum_{j=1}^{n_{\text{SMP}}} \sum_{h=1}^{H} (z_{j,t,h} P_{\text{SMP},h} - z_{j,t,h_{0}} P_{\text{SMP},h_{0}})$$
 (35)

$$\Delta CC_{\text{SMP}} = \sum_{t=2}^{T} \sum_{j=1}^{n_{\text{SMP}}} \sum_{h=1}^{H} C_{\text{SMP}} |z_{j,t,h} - z_{j,t-1,h}| - \sum_{t=2}^{T} \sum_{j=1}^{n_{\text{SMP}}} \sum_{h=1}^{H} C_{\text{SMP}} |z_{j,t,h_0} - z_{j,t-1,h_0}|$$
(36)

$$\Delta CS_{\rm SMP} = 0 \tag{37}$$

$$RE_{\text{SMP}} = w_1 | P_{\text{SMP}, t_1} - P_{\text{SMP}, t_1, 0} | + w_2 | P_{\text{SMP}, t_2} - P_{\text{SMP}, t_2, 0} |$$
 (38)

where C_{SMP} is the cost coefficient of the switching action of SMP.

Once the temperature of the EAF decreases, it takes a large amount of energy and time to reheat to the effective temperature range, thereby incurring substantial economic and time costs. Hence, the EAF must select an operation mode, as specified in (39). Each heat consumes the same amount of energy in the melting process, utilizing the consumed energy to guarantee the generated heat amount, as shown in (40).

$$\sum_{h=1}^{H} z_{j,t,h} = 1 \tag{39}$$

$$\sum_{t=1}^{T} P_{\text{SMP},t} = \sum_{t=1}^{T} P_{\text{SMP},t,0}$$
 (40)

Heat generation occurs in one furnace at a time, rather than continuously adding and outputting new intermediate products, which ensures the integrity of the melting process, as specified in (41).

$$(z_{j,t,h} - z_{j,t-1,h}) + (z_{j,\Theta_h+t-1,h} - z_{j,\Theta_h+t,h}) \le 1$$
(41)

where the subscript Θ_h denotes the melting process corresponding to $P_{\mathrm{SMP},h}$.

Two equipment and a single resource storage unit are configured. If the production rate of EAF is larger than the consumption rate of AOD, the resources are stored. Otherwise, the AODs remain on standby until the storage unit is full. The EAFs share a large storage unit, which increases the potential for coordination. To reduce the calculation complexity, even though the intermediate product of the EAF is produced in a single furnace, it is amortized over the melting time of that furnace. The average value is obtained by dividing the total amount by the period, thereby expressing the production rate, as shown in (42) and (43). The quantity of materials within the storage unit must not exceed its capacity. Otherwise, an overflow of intermediate products may occur, thereby interfering with the normal operation of the subsequent process. Equations (44) and (45) express the constraints.

$$\bar{g}_{j,t} = \sum_{h=1}^{H} \frac{z_{j,t,h} g_h}{\Theta_h} \tag{42}$$

$$G_t = \sum_{i=1}^{n_{\text{SMP}}} \bar{g}_{j,t}$$
 (43)

$$S_t = S_{t-1} + G_t - \tau_{S} \tag{44}$$

$$S_{\text{low}} \leq S_t \leq S_{\text{high}} \tag{45}$$

where $\bar{g}_{j,t}$ is the average production rate of the j^{th} EAF at time t; g_h is the generation rate of the EAF in the h^{th} tap position; G_t is the overall production rate of all EAFs at time t; $\tau_{\rm S}$ is the consumption rate of the EAF; and S_t , $S_{\rm low}$, and $S_{\rm high}$ are the storage capacity at time t, the maximum storage capacity of the storage unit, and the minimum storage capacity of the storage unit, respectively.

Once again, improving SMP operation is not the primary objective, and the regulation scope is constrained by (46) and (47).

$$P_{\text{SMP},t,0} - \delta_{\text{SMP}} \leq P_{\text{SMP},t} \leq P_{\text{SMP},t,0} + \delta_{\text{SMP}} \quad t \in \mathbb{T} \setminus \{t_1, t_2\} \quad (46)$$

$$P_3 \le P_{\text{SMP},t} - P_{\text{SMP},t,0} \le 0 \quad \forall t = t_1, t_2$$
 (47)

where δ_{SMP} is the allowable range of power variation of SMP; and P_3 is the maximum regulation amplitude.

IV. IMPROVED DR POTENTIAL ESTIMATION MODEL CONSIDERING UNCERTAIN AND SUBJECTIVE FACTORS

In Section III, the DR potential of industrial user is estimated on the basis of a comprehensive understanding of the operation status and the incentive price provided by the DSO. In practice, the DR potential estimation is typically performed on day-ahead or periodic basis (e. g., weekly). However, in the actual DR potential estimation process, uncertain and subjective factors arise, such as those associated with unknown parameters, uncertain incentive prices, and psychological factors.

A. Virtual Data Acquisition Method

Specific process arrangements are used in the actual DR potential estimation process. However, these are private parameters and are not reported during DR. The inaccessibility

of these parameters directly affects the accuracy and feasibility of the proposed estimation method. Therefore, a virtual data acquisition method is proposed to reduce the need for the above-mentioned data.

According to (1), ΔCE_s and RE_s are not related to the specific process arrangements, whereas ΔCC_s and ΔCS_s are strongly related to them. However, both ΔCC_s and ΔCS_s subtract the cost of the original operation point from the cost of normal operation and rescheduled operation point. Since the production process is scheduled in advance, the cost of the normal operation is fixed. During optimization, a change to a fixed value in the objective function does not affect the final results, i.e., the original production arrangement does not affect the DR effect after rescheduling.

Therefore, it is not necessary to obtain the original actual data. Thus, obtaining a virtual production arrangement is beneficial. When obtaining a virtual production arrangement, the deviations between the virtual power curve and the original power curve must be minimized, as specified in (48) and (49). The other constraints are the same as those shown in Section III.

$$\min |P_{s,t} - P_{L,s,t}| \tag{48}$$

s.t.

$$(1 - \kappa_1) \sum_{t=1}^{T} P_{L,s,t} \le \sum_{t=1}^{T} P_{s,t} \le (1 + \kappa_2) \sum_{t=1}^{T} P_{L,s,t}$$
 (49)

where $P_{s,t}$ and $P_{L,s,t}$ are the original power and virtual power of industrial user s at time t, respectively; and κ_1 and κ_2 are the constant coefficients used to limit the deviation range, where $\kappa_1 = \kappa_2 = 2\%$.

The virtual data acquisition method for obtaining virtual parameters involves replacing certain inaccessible actual data with logically consistent virtual data. The obtained virtual data may not affect the subsequent DR potential estimation results because the independent constants do not influence the final optimization outcome in the problem-solving process. However, the virtual data acquisition method still requires preliminary data.

B. Considering Uncertain and Subjective Factors

1) Industrial User Participation Threshold

Industrial users who participate in DR are motivated by economic considerations. In contrast to residential users, industrial users have a certain participation threshold when participating in DR, which is related to their specific response characteristics.

- 1) Lower sensitivity to the incentive price. Industrial production involves specific production goals, and ensuring noninterference with normal output is a necessary prerequisite for participation in DR. When participating in DR, the industrial user (plant) must adjust its production processes, which incurs additional costs. Therefore, industrial users are relatively insensitive to incentives and are unlikely to adjust their production processes in response to small changes in incentives.
- 2) Higher participation intention threshold. The electricity cost of the industrial production is significant. If participating in DR yields only small economic revenues, the industrial user is more likely to maintain the original operation sta-

tus

- 3) Indirect response mode. Generally, residential users switch the operation status or adjust the operation parameters to directly change their current power consumption. Industrial users are inclined to adjust the production process due to production sequence and targets, which indirectly alters their power consumption, as shown in Supplementary Material A Figs. SA1 and SA2.
- 4) Significant response effect. Industrial users have advantages in response amplitude and duration compared with residential users.

Based on the response characteristics of industrial users, an industrial user participation threshold is proposed to judge whether the industrial user is willing to participate in DR, as shown in Fig. 3.

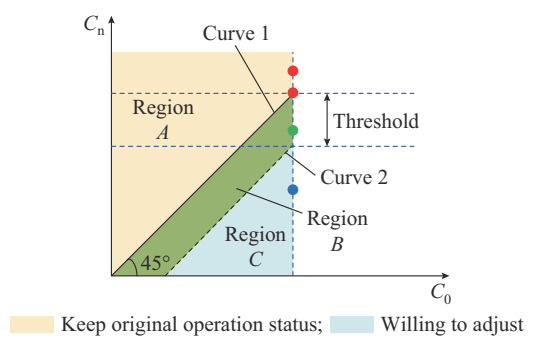


Fig. 3. Judgment of industrial user's willing to participate in DR.

Let C_0 and C_n represent the cost of the industrial user in normal operation status and that after participating in DR, respectively. As shown in Fig. 3, the two curves divide the plane into three regions. Region A represents the case where $C_n > C_0$. Region B represents the case where $C_n < C_0$, but $C_n - C_0$ is smaller than the proposed threshold. Region C indicates that $C_n - C_0$ is larger than the proposed threshold. Furthermore, the DR behavior of the industrial user under different conditions can be identified. Specifically, only when the changes in costs fall within Region C will the industrial user adjust its production process. In other words, only the blue point in Fig. 3 represents the case where the industrial user is willing to adjust the production process, which means that the industrial user is willing to participate in DR.

$$\begin{cases} C_n - C_0 \le -TLV & \text{Willing to participate in DR} \\ C_n - C_0 > -TLV & \text{Unwilling to participate in DR} \end{cases}$$
 (50)

where TLV is the proposed threshold, and TLV > 0.

The theoretical value of the proposed threshold can be determined based on the proportion of the average annual revenue of the industry and the ratio of the electricity bill to total costs. In practical applications, the theoretical value can be adjusted according to other factors, such as the current production demand, production schedules, and seasonal profitability.

The setting of the theoretical value aligns with the actual choices of industrial users, as they are unlikely to alter their original operation status for small revenues. Industrial users of different types and sizes exhibit varying proposed thresholds.

2) Incentive Price and Bounded Rationality

The proposed threshold assists industrial users in determining whether to participate in DR. However, the index used by industrial users to determine whether to participate in DR is not based on absolute costs, but rather on perceived costs. Absolute costs refer to the revenue an industrial user would receive in a known situation with perfect rationality. This estimation environment is difficult to achieve due to the bounded rationality of industrial users and the incentive prices. It is worth noting that the incentive price is one of the uncertain factors and the bounded rationality is one of the subjective factors.

In this context, industrial users can only receive perceived costs and make decisions based on incentive price and bounded rationality. Influenced by irrational psychological factors, industrial users with varying levels of rationality make different choices. Prospect theory (PT) [26] is a theory that can accurately model the irrational behaviors of industrial users and describe and predict the behavior of individuals in risk decision-making processes. PT differs from traditional expected-value theory and expected-utility theory in converting the objective probability of users into subjective probability.

PT assumes that the risk decision-making process consists of an editing process and an estimation process. In the editing process, industrial users with bounded rationality define their revenues and losses using the proposed threshold as a reference point. In the DR potential estimation process, industrial users evaluate each edited prospect and choose the best option based on the value function and weighting function

Editing process: in many DR markets (e.g., in China), industrial users are required to report their DR potential estimation in advance, after which the incentive price is provided. If the incentive price exceeds the expectation, the revenue is greater. Otherwise, the industrial user may incur a loss. In this case, the industrial user is more likely to report a stable value based on historical incentive prices. Determining how to estimate the DR potential under conditions of uncertainty and improve economic performance in most cases is worth studying.

An improved DR potential estimation model considering incentive price is proposed. The variable $(\Omega, \Delta P_{s,t_1}, \Delta P_{s,t_2})$ denotes that the incentive price is Ω and the response amplitude is $(\Delta P_{s,t_1}, \Delta P_{s,t_2})$. Equation (51) calculates the actual revenue of the industrial user $V_s(\tilde{\Omega}, \Delta P_{s,t_1}, \Delta P_{s,t_2})$ when the given incentive price is $\tilde{\Omega}$, while the industrial user obtains the reported $(\Delta P_{s,t_1}, \Delta P_{s,t_2})$ based on Ω . The first two terms $\tilde{\Omega}$ and $\Delta P_{s,t_1}$ calculate the actual cost when the industrial user participates in DR with $(\Omega, \Delta P_{s,t_1}, \Delta P_{s,t_2})$. The third term $\Delta P_{s,t_2}$ calculates the revenue deviation. Considering the characteristic of lower sensitivity to the incentive price, it is easy to obtain $(\Delta P_{s,t_1}, \Delta P_{s,t_2})$ with different Ω , and $(\Delta P_{s,t_1}, \Delta P_{s,t_2})$ has a limited number of levels.

$$\begin{split} V_{s}(\tilde{\mathcal{Q}}, \Delta P_{s,t_{1}}, \Delta P_{s,t_{2}}) = -[C_{s}(\mathcal{Q}, \Delta P_{t_{1}}, \Delta P_{t_{2}}) + (1 - \lambda_{s}) \\ \Delta CE_{s}(\mathcal{Q}, \Delta P_{t_{1}}, \Delta P_{t_{2}}) - (\tilde{\mathcal{Q}} - \mathcal{Q})(\Delta P_{t_{1}} + \Delta P_{t_{2}})] \end{split} \tag{51}$$

Estimation process: the actual load curve and incentive price are uncertain factors that affect the DR potential estimation. As day-ahead forecasting achieves a high degree of accuracy and industrial users exhibit lower sensitivity to incentive prices, small power fluctuations in the load curve do not interfere with response decisions. Therefore, only the uncertainty of the given incentive prices is considered. Two key functions are explored: the value function and the weighting function.

Equation (52) infers the perceived costs of industrial user s in the specified response amplitude ($\Delta P_{s,t_1}, \Delta P_{s,t_2}$) based on the probability distribution of historical incentive prices. Furthermore, (52) can be discretized to (53) to reduce the difficulty of the solution.

$$\tilde{V}_{s}(\Delta P_{s,t_{1}}, \Delta P_{s,t_{2}}) = \int_{\tilde{O} \in \mathcal{R}} V_{s}(\tilde{Q}, \Delta P_{s,t_{1}}, \Delta P_{s,t_{2}}) \rho(\tilde{Q})$$
 (52)

$$\tilde{V}_{s}(\Delta P_{s,t_{1}}, \Delta P_{s,t_{2}}) = \sum_{\tilde{\Omega} \in \mathcal{R}} V_{s}(\tilde{\Omega}, \Delta P_{s,t_{1}}, \Delta P_{s,t_{2}}) \rho(\tilde{\Omega})$$
 (53)

where $\tilde{V}_s(\Delta P_{s,t_1}, \Delta P_{s,t_2})$ is the perceived cost of industrial user s as the value function when the response amplitude is $(\Delta P_{s,t_1}, \Delta P_{s,t_2})$; $\rho(\tilde{\Omega})$ is the probability of $\tilde{\Omega}$ and $\sum_{\tilde{\Omega} \in \mathcal{R}} \rho(\tilde{\Omega}) = 1$; and \mathcal{R} is the set of feasible incentive prices.

Moreover, industrial users are not always perfectly rational but more often exhibit bounded rationality, which leads to varying risk preferences. $\rho(\tilde{\Omega})$ is the objective function that maps the perfectly rational situation, while $\omega(\rho(\tilde{\Omega}))$ is the corresponding subjective probability. According to [27], $\omega(\rho(\tilde{\Omega}))$ is the probability weighting function that transforms objective probabilities into subjective probabilities, as defined in (54). When rationality degree α is set to be 1, industrial users are perfectly rational. When α decreases, industrial users become more inclined to the occurrence of low-probability events. The value of α can be obtained through field research or analysis of the historical behavioral data.

$$\omega(\rho(\tilde{\Omega})) = \exp\left[-(-\ln \rho(\tilde{\Omega}))^{\alpha}\right] \quad 0 \le \alpha \le 1$$
 (54)

The S-shaped value function $\tilde{V}_s(\Delta P_{s,t_1}, \Delta P_{s,t_2})$ indicates that an industrial user exhibits risk-seeking behavior when facing losses and risk-averse behavior when dealing with revenues. Therefore, the objective function in (1) is modified as:

$$\tilde{V}_{s}(\Delta P_{s,t_{1}}, \Delta P_{s,t_{2}}) = \omega(\rho(\tilde{\Omega})) \sum_{\tilde{\Omega} \in \mathcal{R}} V_{s}(\tilde{\Omega}, \Delta P_{s,t_{1}}, \Delta P_{s,t_{2}})$$
 (55)

When confronted with different values of Ω , the industrial user exhibits varying DR effects. The objective function (1) provides the optimal DR behavior of industrial users under deterministic Ω . Considering the bounded rationality of industrial users and the uncertainty of actual Ω , the S-shaped value function (55) formulated based on PT and (1) describes the perceived costs of industrial user DR behavior under uncertain Ω . However, this perceived cost only represents the revenue from the current DR behavior, but not the overall DR behavior. Nevertheless, the goal of DR potential

estimation is to determine the response amplitude through economic optimization. Therefore, additional process is needed

The set of all DR behaviors $P_s = \{(\Delta P_{s,t_1,1}, \Delta P_{s,t_2,1}), (\Delta P_{s,t_1,2}, \Delta P_{s,t_2,2}), ..., (\Delta P_{s,t_1,2}, \Delta P_{s,t_2,2}), ..., (\Delta P_{s,t_1,Z}, \Delta P_{s,t_2,Z})\}$ is obtained through (1), where subscript z denotes the z^{th} DR behavior; and Z is the last DR behavior. The obtained $\tilde{V}_s(\Delta P_{s,t_1,z}, \Delta P_{s,t_2,z})$ is defined as a prospect set. Correspondingly, the prospect \tilde{V}_s can be obtained. Among all the prospect sets, the industrial user may choose the DR capacity corresponding to the best prospect $(\Delta P_{s,t_1}^*, \Delta P_{s,t_2}^*)$ as the DR potential estimation. Therefore, the improved DR potential estimation model is expressed as:

$$\begin{cases} \max \tilde{V}_{s}(\Delta P_{s,t_{1},z}, \Delta P_{s,t_{2},z}) \\ \text{s.t. } (2)\text{-}(47) \\ (\Delta P_{s,t_{1},z}, \Delta P_{s,t_{2},z}) \in P_{s} \end{cases}$$

$$(56)$$

Finally, the industrial user determines whether to participate in DR according to the perceived costs. Therefore, the reported potential capacity $(\Delta P_{s,t_1}^*, \Delta P_{s,t_2}^*)$ of industrial user s can be derived as:

$$(\Delta P_{s,t_1}^*, \Delta P_{s,t_2}^*) = \begin{cases} (\Delta P_{s,t_1}^*, \Delta P_{s,t_2}^*) & \tilde{V}_s (\Delta P_{s,t_1}^*, \Delta P_{s,t_2}^*) \ge TLV_s \\ (0,0) & \tilde{V}_s (\Delta P_{s,t_1}^*, \Delta P_{s,t_2}^*) < TLV_s \end{cases}$$
(57)

V. CASE STUDY

In this section, DR potential estimations of the ASP, CMP, and SMP are calculated. The actual load curves and electricity price data over three months are obtained from an industrial park in China. Parameter settings are listed in Table I.

TABLE I PARAMETER SETTINGS

Parameter	Value	Parameter	Value
Φ (MW)	2.2	$P_{ASP,k}$ (MW)	18, 19, 20
Θ_h	4, 3, 2	$P_{SMP,h}$ (MW)	22.5, 30.0, 40.0
$\tau_{\rm S}, \tau_{\rm M} \left(t \right)$	180, 4	$P_1, P_2, P_3 \text{ (MW)}$	12, 10, 25
$B_{ m p}$	0.25	$q_1(t)$	10
C_{ASP} , C_{SMP} , C_{CMP} (\$)	90, 150, 180	$Q_{\mathrm{low}}, Q_{\mathrm{high}} (t)$	0, 20
$\bar{g}(t)$	22.5, 30.0, 40.0	$S_{_{1}}$ (t)	100
H	3	$S_{\text{low}}, S_{\text{high}}(t)$	0, 3000
K	3	T	48
$n_{\mathrm{ASP}}, n_{\mathrm{CMP}}, n_{\mathrm{SMP}}$	15, 30, 6	w₁, w₂ (\$·MWh)	120, 120

A. Correlation Analysis

In Supplement Material A Fig. SA3, the first column shows the HD between daily loads in a specified plant and the second column shows the HD between daily loads and the electricity price in a specified plant. In addition, rows 1-3 show the calculated HDs of ASP, CMP, and SMP, respectively. Based on Fig. SA3 and Table II, the daily load of the same industrial user exhibits a strong correlation. The simi-

larity between workday load curvers and nonworkday load curvers is high, indicating similar operation patterns. Therefore, the proposed estimation model can be used to estimate the DR potential of a specified industrial user, regardless of workdays or nonworkdays. In addition, industrial power consumption and electricity prices are related, but their similarity is weaker than that between daily loads. Thus, industrial power consumption is affected by the electricity price, but the electricity price is not the decisive factor that affects the production process. Therefore, it is reasonable to weaken the influence of electricity cost variation factors in the proposed estimation model.

TABLE II COMPARISON OF HDS

Industrial — user		HD	
	Workday v.s. workday	Workday v.s nonworkday	Load curve v.s electricity price
ASP	3.42	3.48	5.04
CMP	2.66	2.69	6.25
SMP	2.82	2.88	5.28

B. Validation of Proposed Estimation Model

The proposed estimation model is applied to ASP, CMP, and SMP to validate its effectiveness under different cases. This subsection outlines the DR effects of different industrial users under various incentive prices, categorized as cases 1, 2, and 3. To demonstrate the significant stepwise DR effects, the incentive prices chosen in ASP are divided into three levels: \$60, \$90, and \$120. The other two industrial users selected incentives of \$40, \$60, and \$80. The comparison of specific revenue is listed in Table III, and the DR effects are detailed below.

TABLE III
COMPARISON OF REVENUES

Case No		Revenue (\$)	
	ASP	CMP	SMP
1	2814.0	-6849.6	20931
2	4293.2	-5556.6	21681
3	5720.9	-4999.6	22899

1) ASP

Taking the ASP response as an example, Figs. 4 and 5(a)-(c) are compared. It is worth noting that different colors in Fig. 5 represent different tap positions. Since Fig. 5 is only for overall visual comparison rather than detailed comparison, there is no legend. As shown in Fig. 4, the greater the incentive price, the larger the response amplitude. As the incentive price increases, switching the operation status becomes more complicated. Only when the incentive price is large enough to cover the cost of switching may the ASP be inclined to response in order to gain more revenues. Under the constraint of λ_{ASP} , the operation status of the ASP still follows certain operational rules. Table III compares the revenues of the ASP under different incentive prices. Under a reasonable arrangement of production process, the greater

the response amplitude, the greater the obtained revenues, which aligns with conventional understanding.

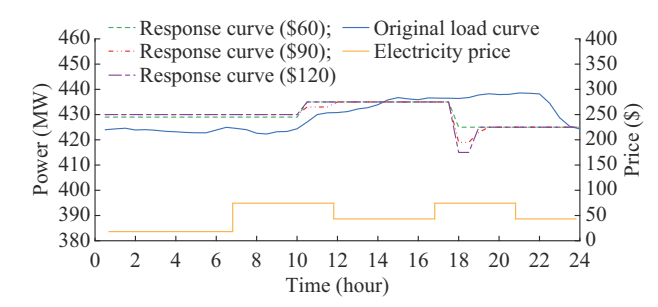


Fig. 4. Comparison of response performance of ASP under different incentive prices.

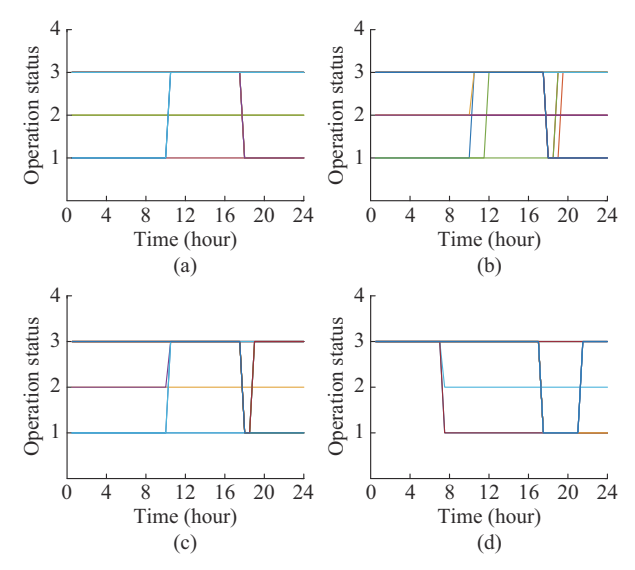


Fig. 5 Comparison of tap positions of ASP. (a) Incentive price is set to be \$60. (b) Incentive price is set to be \$90. (c) Incentive price is set to be \$120. (d) Incentive price is set to \$60 without setting λ_{ASP} .

Figures 5(a), 5(d), and 6 are compared to demonstrate the necessity of the introduction of λ_{ASP} . The weighted electricity cost is not considered in the residential load response. In addition, the electricity cost is negligible compared with the obtained response revenue. However, industrial users consume large amounts of electricity, and the electricity cost and response revenue are not on the same order of magnitude.

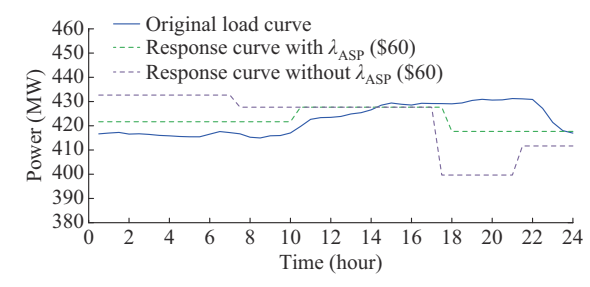


Fig. 6. Comparison of response performance of ASP with and without λ_{ASP} .

If λ_{ASP} is not introduced, the ASP will prioritize economic factors excessively. This leads to a substantial increase in the disparity of power consumption across different periods, thereby causing the operation of the ASP to deviate from its

normal operational rules, as depicted in Fig. 6. 2) *CMP*

Figure 7 shows the comparison of response performance of CMP under different incentive prices.

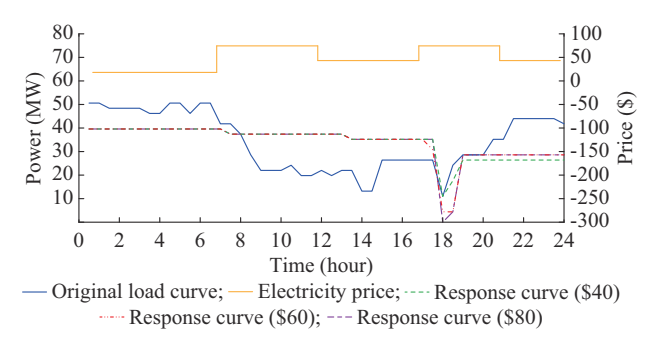


Fig. 7. Comparison of response performance of CMP under different incentive prices.

The difference between the CMP response curve and the ASP response curve is that when the incentive price exceeds a certain value, the response effect is significantly enhanced. This occurs due to the fact that, around this value, the costs and revenues are roughly balanced. When the incentive price increases significantly, the revenues outweigh the cost change, and the CMP is more likely to response and obtain greater revenues. However, the revenues in Table III indicate that CMP consistently shows negative revenues. Therefore, the evaluated CMP may never participate in DR. This is because, despite having theoretical DR potential, its economic DR potential is zero. Therefore, it is necessary to select other CMPs or industrial users as participants in the response process.

Figure 8 shows the comparison of the salary and employment costs of a CMP under different incentive prices. The peaks and valleys of salary and electricity prices are inversely related. Through strategic planning, salary expenditures can be reduced by adjusting the pace of power consumption.

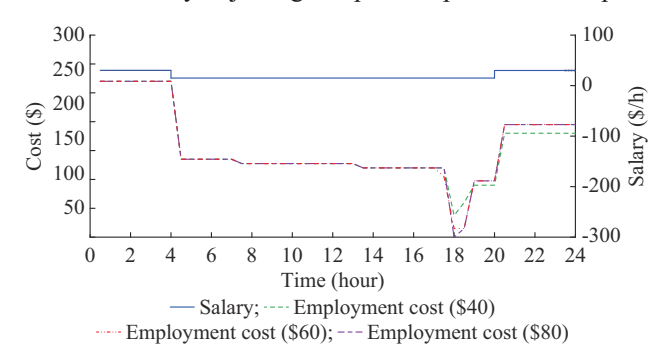


Fig. 8. Comparison of salary and employment costs of CMP under different incentive prices.

Figure 9 shows the comparison of effects of the storage capacity on CMP response (incentive price is set to be \$60). Changing the storage capacity affects the response curve but not the response amplitude. This is because there is still some room for a CMP to respond at low storage capacities. Therefore, changes in the storage capacity within a certain range do not affect the response performance.

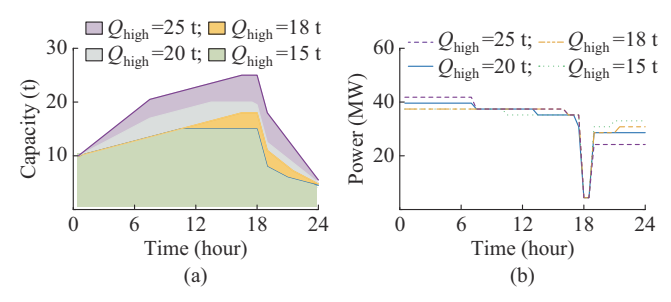


Fig. 9. Comparison of effects of storage capacity on CMP response (incentive price is set to be \$60). (a) Capacity evolution under different storage capacities. (2) Response effects under different storage capacities.

3) SMP

Figure 10 shows the comparison of the response performance of an SMP under different incentive prices. Figure 11 shows the comparison of effects of initial storage capacity on SMP response (incentive price is set to be \$60). The difference between the initial storage capacity and storage capacity is that the overall response curve is unaffected when the storage capacity is sufficient. Storage capacity affects the response curve because a change in storage capacity alters the overall planning space, giving the industrial user various choices. As shown in Table III, among three industrial users, the SMP has the highest unit response revenue and the largest response range, making it a reliable and efficient choice for DR participation.

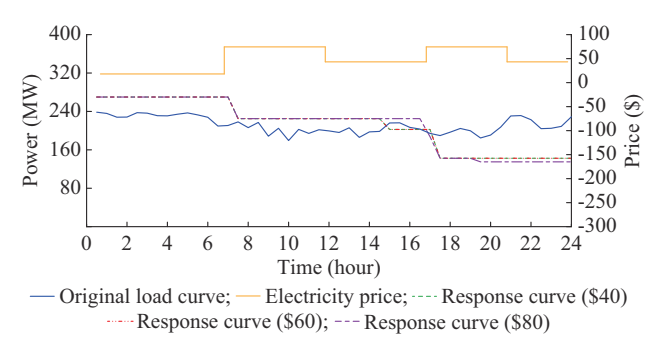


Fig. 10. Comparison of response performance of SMP under different incentive prices.

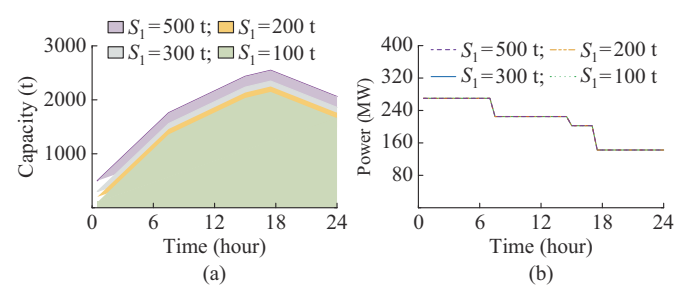


Fig. 11. Comparison of effects of initial storage capacity on SMP response (incentive price is set to be \$60). (a) Capacity evolution under different initial storage capacities. (2) Response effects under different initial storage capacities.

4) Validation of Virtual Data Acquisition Method

In this study, the improved DR potential estimation model is adopted by three industrial users. To reduce redundancy, the ASP is used as an example for verification as follows.

Figure 12 compares the actual load curve with the fitted load curve, showing that the errors between the two curves are small. The parameters obtained during curve fitting are incorporated into the proposed estimation model for the same calculation. A comparison of Fig. 4 and Supplementary Material A Fig. SA4 shows that the final DR potential estimation obtained using the fitted load curve is identical to that obtained using the known actual load curve. Therefore, the virtual data acquisition method further reduces the difficulty in data acquisition and effectively protects the industrial user privacy.

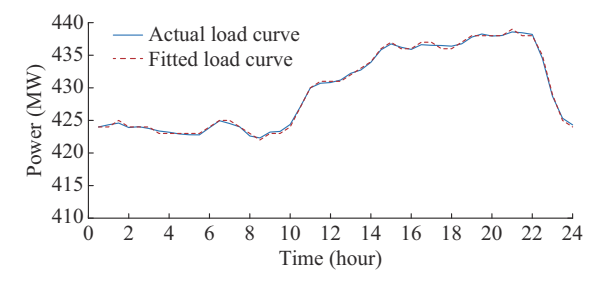


Fig. 12. Comparison of actual load curve and fitted load curve.

5) Validation of Uncertain and Subjective Factors

The industrial user infers the incentive price that the DSO may offer based on the previous rule, and accordingly determines the optimal response behavior, thereby obtaining $V_s(x)$. Figure 13 shows the industrial user perceived costs of PT under different rationality degrees. The values for CMP and SMP in Fig. 13 are the actual values divided by 10 to maintain the balance of the figure.

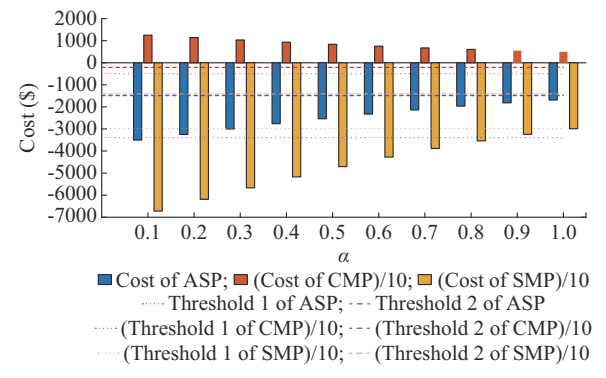


Fig. 13. Industrial user perceived costs of PT under different rationality degrees.

According to Fig. 13, when the rationality degree of industrial user is low, the expectation for the future tends to be overly optimistic, and the expected revenue is much greater than the actual possible revenue. In this case, the DSO yields a positive response with a low incentive price, but this may negatively affect the user.

As depicted in Fig. 13, two proposed thresholds (threshold 1 and threshold 2) are presented. Among them, the value of threshold 2 is excessively small, rendering the rationality of users ineffective in determining whether to participate in DR. However, with the setting of threshold 2, industrial users with low rationality may participate in DR due to overly optimistic revenue estimates. Despite this, the actual expected revenue cannot support their participation. That is, the

threshold is not actually met, but the user participates given the optimistic estimate. Therefore, it leads to a false response.

Moreover, the CMP may not participate in DR, regardless of whether threshold 1 or threshold 2 is adopted, whereas the ASP and SMP responses are directly related to the selection of the threshold. The selection of the threshold is important: a large threshold is not conducive to DR participation and may lead to false responses. As shown in Supplementary Material A Fig. SA5, there are fewer ASP false responses, but the proportion of SMP false responses is high. Nonetheless, while the selection of a relatively small threshold can decrease the probability of false responses, it may lead to frequent DR participation, which has the potential to impact normal production. In Fig. SA6 of Supplementary Material A, both ASP and SMP participate in DR, regardless of the rationality degree of the industrial user.

Therefore, industrial users should select the thresholds based on their specific circumstances, ensuring that they are neither too small to have a meaningful impact nor too large to negatively affect their revenues and response performance.

6) Validation of Actual Data

The proposed estimation model is applied to simulate the actual response effect using DR data from an SMP. Taking a response event in 2022 as an example, and the compensation price is set to be 2.3 \(\frac{4}{k}\)Wh according to the "Demand Response Management Guidelines". With the proposed estimation model, the response revenue of the ASP exceeds the proposed threshold, indicating the willingness to participate in DR. As shown in Fig. 14, the overall response effect is aligned well, confirming the effectiveness and accuracy of the proposed estimation model.

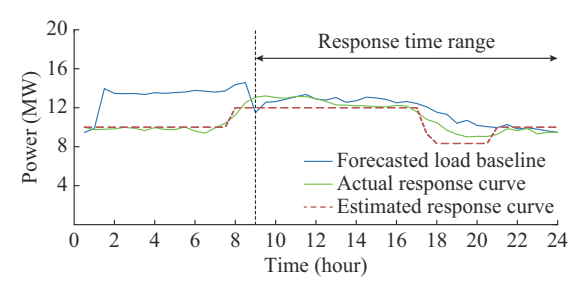


Fig. 14. Validation of actual data of SMP.

VI. CONCLUSION

A unified DR potential estimation model based on PT for typical industrial users is proposed. The uncertainty of parameters and the rationality of industrial users significantly impact the decision-making progress, influencing both the effect and the economy of participation, as well as determining whether industrial users are willing to participate in DR. For industrial users, the decision to participate in DR forms the basis for estimating the effects of participation.

The simulation results demonstrate that the proposed estimation model can accurately estimate the DR potential of various industrial users. Furthermore, the estimated storage capacity, derived from combining the proposed threshold and the risk attitudes of the users toward uncertain and subjective factors, holds practical significance and provides valuable guidance to the response behavior of users participating

in DR. When the rationality degree of the industrial user is low, industrial users are more willing to participate in DR under the same conditions. Finally, when data is limited, the virtual data acquisition method facilitates the completion of the estimation process.

In summary, the proposed estimation model effectively estimates DR potential for typical industrial users with consideration of uncertain and subjective factors.

REFERENCES

- [1] M. Shafie-khah, P. Siano, J. Aghaei et al., "Comprehensive review of the recent advances in industrial and commercial DR," *IEEE Transac*tions on Industrial Informatics, vol. 15, no. 7, pp. 3757-3771, Jul. 2019
- [2] B. Surampudy, M. Keller, and T. Gibson. (2019, Dec.). 2019 utility demand response market snapshot. [Online]. Available: https://sepapower.org/resource/2019-utility-demand-response-market-snapshot/
- [3] Y. Wang, Q. Chen, T. Hong et al., "Review of smart meter data analytics: applications, methodologies, and challenges," *IEEE Transactions on Smart Grid*, vol. 10, no. 3, pp. 3125-3148, May 2019.
- [4] Y. Zhang, Q. Wu, Q. Ai et al., "Closed-loop aggregated baseline load estimation using contextual bandit with policy gradient," *IEEE Trans*actions on Smart Grid, vol. 13, no. 1, pp. 243-254, Jan. 2022.
- [5] L. Zhang, G. Li, Y. Huang et al., "Distributed baseline load estimation for load aggregators based on joint FCM clustering," *IEEE Transac*tions on Industry Applications, vol. 59, no. 1, pp. 567-577, Jan. 2023.
- [6] K. Li, Y. Wang, N. Zhang et al., "Precision and accuracy co-optimization-based demand response baseline load estimation using bidirectional data," *IEEE Transactions on Smart Grid*, vol. 14, no. 1, pp. 266-276. Jan. 2023.
- [7] K. Li, J. Yan, L. Hu et al., "Two-stage decoupled estimation approach of aggregated baseline load under high penetration of behind-the-meter PV system," *IEEE Transactions on Smart Grid*, vol. 12, no. 6, pp. 4876-4885, Nov. 2021.
- [8] D. Muthirayan, E. Baeyens, P. Chakraborty et al., "A minimal incentive-based demand response program with self reported baseline mechanism," *IEEE Transactions on Smart Grid*, vol. 11, no. 3, pp. 2195-2207, May 2020.
- [9] K. Baek, E. Lee, and J. Kim, "Resident behavior detection model for environment responsive demand response," *IEEE Transactions on Smart Grid*, vol. 12, no. 5, pp. 3980-3989, Sept. 2021.
- [10] T. Jiang, P. Ju, C. Wang et al., "Coordinated control of air-conditioning loads for system frequency regulation," *IEEE Transactions on Smart Grid*, vol. 12, no. 1, pp. 548-560, Jan. 2021.
- [11] G. Ruan, D. S. Kirschen, H. Zhong et al., "Estimating demand flexibility using Siamese LSTM neural networks," *IEEE Transactions on Power Systems*, vol. 37, no. 3, pp. 2360-2370, May 2022.
- [12] N. Gerami, A. Ghasemi, A. Lotfi et al., "Energy consumption modeling of production process for industrial factories in a day ahead scheduling with demand response," Sustainable Energy, Grids and Networks, vol. 25, p. 100420, Mar. 2021.
- [13] M. Paulus and F. Borggrefe, "The potential of demand-side management in energy-intensive industries for electricity markets in Germany," *Applied Energy*, vol. 88, no. 2, pp. 432-441, Feb. 2011.
- [14] S. T. Taleghani, M. Sorin, and S. Gaboury, "Thermo-economic analysis of heat-driven ejector system for cooling smelting process exhaust gas," *Energy*, vol. 220, p. 119661, Apr. 2021.
- [15] H. Golmohamadi, R. Keypour, B. Bak-Jensen et al., "Robust self-scheduling of operational processes for industrial demand response aggregators," *IEEE Transactions on Industrial Electronics*, vol. 67, no. 2, pp. 1387-1395, Feb. 2020.
- [16] J. Wang, Y. Shi, and Y. Zhou, "Intelligent demand response for industrial energy management considering thermostatically controlled loads and EVs," *IEEE Transactions on Industrial Informatics*, vol. 15, no. 6, pp. 3432-3442, Jun. 2019.
- pp. 3432-3442, Jun. 2019.
 [17] Y. Zheng, W. Zhao, M. Varga et al., "Stochastic energy management of large industrial-scale aquaponics considering robust optimization-based demand response program," Applied Energy, vol. 374, p. 123982, Nov. 2024.
- [18] Y. Wu, Z. Lin, C. Liu et al., "A demand response trade model considering cost and profit allocation game and hydrogen to electricity conversion," *IEEE Transactions on Industry Applications*, vol. 58, no. 2, pp. 2909-2920, Mar. 2022.

- [19] R. Lu, R. Bai, Y. Huang et al., "Data-driven real-time price-based demand response for industrial facilities energy management," Applied Energy, vol. 283, p. 116291, Feb. 2021.
- [20] L. Silvestri and M. De Santis, "Renewable-based load shifting system for demand response to enhance energy-economic-environmental performance of industrial enterprises," *Applied Energy*, vol. 358, p. 122562, Mar. 2024.
- [21] W. Zhao, K. Ma, J. Yang et al., "A multi-time scale demand response scheme based on noncooperative game for economic operation of industrial park," *Energy*, vol. 302, p. 131875, Sept. 2024.
- [22] X. Huang, S. H. Hong, and Y. Li, "Hour-ahead price based energy management scheme for industrial facilities," *IEEE Transactions on In*dustrial Informatics, vol. 13, no. 6, pp. 2886-2898, Dec. 2017.
- [23] X. Zhang, G. Hug, and I. Harjunkoski, "Cost-effective scheduling of steel plants with flexible EAFs," *IEEE Transactions on Smart Grid*, vol. 8, no. 1, pp. 239-249, Jan. 2017.
- [24] Y. Wen and W. Zhang, "A minimax model for generalized penetration distance between convex sets by directed Hausdorff distance," *IEEE Robotics and Automation Letters*, vol. 7, no. 3, pp. 6123-6130, Jul. 2022
- [25] X. Zhang and G. Hug, "Optimal regulation provision by aluminum smelters," in *Proceedings of 2014 IEEE PES General Meeting | Con*ference & Exposition, National Harbor, USA, Jul. 2014, pp. 1-5.
- [26] W. Chen, J. Qiu, and Q. Chai, "Customized critical peak rebate pricing mechanism for virtual power plants," *IEEE Transactions on Sustainable Energy*, vol. 12, no. 4, pp. 2169-2183, Oct. 2021.
- [27] D. Prelec, "The probability weighting function," *Econometrica*, vol. 66, no. 3, p. 497, May 1998.

Tingyu Jiang received the B.S. and Ph.D. degrees in electrical engineering from Hohai University, Nanjing, China, in 2017 and 2022, respectively. She is currently a Lecturer at the School of Electrical and Power Engineering, Hohai University. Her research interests include demand response, ancillary service, and game theory application in scheduling.

Chuan Qin received the B.Eng. degree in electrical engineering from Nantong Institute of Technology, Nantong, China, in 2002, and the M.Sc. and Ph.D. degrees in electrical engineering from Hohai University, Nanjing, China, in 2005 and 2013, respectively. He is currently an Associate Profesor at School of Electrical and Power Engineering, Hohai University. His research interests include modeling and control of power system and renewable power generation.

Yuzhong Gong received the B.S. degree from Zhejiang University of Technology, Hangzhou, China, in 2010, and the Ph.D. degree from Zhejiang University, Hangzhou, China, in 2015. He is currently a Research Associate at Zhejiang University. His research interests include power system planning and operation, renewable energy integration, and energy storage system.

Ke Wang received the M. E. degree in electrical engineering from State Grid Electric Power Research Institute, Nanjing, China, in 2004, and the Ph.D. degree in electrical engineering from China Electric Power Research Institute, Beijing, China, in 2018. She is currently a Professor at School of Electrical and Power Engineering, Hohai University, Nanjing, China. Her research interests include demand response scheduling optimization and power system simulation.

Ping Ju received the B.S. and M.S. degrees in electrical engineering from Southeast University, Nanjing, China, in 1982 and 1985, respectively, and the Ph.D. degree in electrical engineering from Zhejiang University, Hangzhou, China, in 1988. From 1994 to 1995, he was an Alexander-von Humboldt Fellow with the University of Dortmund, Dortmund, Germany. He is currently a Professor of Hohai University, Nanjing, China and Zhejiang University, His research interests include modeling and control of power system with integration of renewable generation.

Chi Yung Chung received the B.Eng. (Hons.) and Ph.D. degrees in electrical engineering from The Hong Kong Polytechnic University, Hong Kong, China, in 1995 and 1999, respectively. He is currently the Head of the Department and a Chair Professor in power systems engineering with the Department of Electrical Engineering, The Hong Kong Polytechnic University. His research interests include smart grid technology, renewable energy, power system stability and control, planning and operation, computational intelligence application, power market, and electric vehicle charging.